Conference paper

Katarzyna Rybicka-Jasińska, James B. Derr and Valentine I. Vullev*

What defines biomimetic and bioinspired science and engineering?

https://doi.org/10.1515/pac-2021-0323

Abstract: Biomimicry, biomimesis and bioinspiration define distinctly different approaches for deepening the understanding of how living systems work and employing this knowledge to meet pressing demands in engineering. Biomimicry involves shear imitation of biological structures that most often do not reproduce the functionality that they have while in the living organisms. Biomimesis aims at reproduction of biological structure-function relationships and advances our knowledge of how different components of complex living systems work. Bioinspiration employs this knowledge in abiotic manners that are optimal for targeted applications. This article introduces and reviews these concepts in a global historic perspective. Representative examples from charge-transfer science and solar-energy engineering illustrate the evolution from biomimetic to bioinspired approaches and show their importance. Bioinspired molecular electrets, aiming at exploration of dipole effects on charge transfer, demonstrate the pintail impacts of biological inspiration that reach beyond its high utilitarian values. The abiotic character of bioinspiration opens doors for the emergence of unprecedented properties and phenomena, beyond what nature can offer.

Keywords: Bioinspired; biomimesis; biomimetic; biomimimicry; charge transfer; dipoles; electret; NICE 2020; solar energy.

Introduction

Our planet currently struggles to cope with destructive forces of environmental pollution, waste and increasing amounts of greenhouse gases in the atmosphere. Projections show 6 % rise in CO_2 emissions from energy production in the period between 2015 and 2050, should the current policies be in place. To meet the goals set by the Paris agreement, the world has to reduce the release of CO_2 by more than 29 % [1].

The ever-increasing human population places growing demands for energy, thus, cornering us to expediently make choices for alternative carbon-neutral sources of energy. Current social movements, such as the international school strike for climate (Youth for Climate), bring rising awareness of the challenges for

Article note: A collection of invited papers based on presentations at the 5th International Conference on Bioinspired and Biobased Chemistry and Materials & 2nd International Conference on Optics, Photonics, & Materials (NICE 2020) held in Nice, France and online, Oct. 12–14, 2020.

Katarzyna Rybicka-Jasińska and James B. Derr contributed equally to this work.

***Corresponding author: Valentine I. Vullev**, Department of Biochemistry, University of California, Riverside, CA, 92521, USA; Department of Bioengineering, University of California, Riverside, CA, 92521, USA; Department of Chemistry, University of California, Riverside, CA, 92521, USA; and Materials Science and Engineering Program, University of California, Riverside, CA, 92521, USA, e-mail: vullev@ucr.edu

Katarzyna Rybicka-Jasińska, Institute of Organic Chemistry, Polish Academy of Sciences, Kasprzaka 44/52, 01-224, Warsaw, Poland

James B. Derr, Department of Biochemistry, University of California, Riverside, CA, 92521, USA

the 21st century. Worldwide news of dramatic natural disasters has led to discussions about climate change and the urgent need for action.

While the timely importance of these efforts is paramount, in their extremes they set environmental safety against technological progress. Such ways of thinking do not necessarily lead to constructive discussions and feasible solutions for long-term sustainability. Nature with all living systems represents forms of "technologies" that have evolved for a few billion years. Spinning out of them, human ingenuity has led the development of tools and industries that made us the first living species who have the power to affect the planet, and we did in many different ways. Hence, we do have the knowhow for putting the brakes on environmental pollution and climate change in order to ensure our survival not only as a species but also as a civilization.

Nature offers paradigms for sustainability. Understanding and mimicking the natural systems and the structure-function relationships that governs them is crucial for building a scientific foundation for a sustainable future (Fig. 1). Taking ideas from biology to employ them in bioinspired ways allows for achieving functionalities that are beyond what nature can offer (Fig. 1). Such biological inspiration paves the paths forward to powerful technologies that can meet the growing socio-economic demands of humanity in environmentally benign manners.

Although coal powered the Industrial Revolution in a cost-efficient manner, its use, along with that of other fossil fuels, has led to an exponential increase in CO_2 emissions [2]. The recent emergence of renewable energy technologies, such as solar, hydro, geothermal and wind, offers access to electricity in unprecedented environmentally safe manners [3]. (Strictly speaking, nothing is "renewable", and this term has erroneous denotation in this case. The entropy increase defines the direction of time and turning back to restore states of the Universe the way they were is impossible. Hence, "sustainable energy" is the scientifically correct term, instead.) Among the carbon-neutral energy sources, solar has the incomparable capability to meet our global energy needs. The solar light radiation brings energy to the Earth's surface at rates of 1.76×10^5 TW, and about 1.2×10^5 TW get absorbed when accounting for the global albedo [4]. Utilizing only 0.5 % of this abundant energy source, i.e., at rates of 600 TW, will still meet our global demands for centuries to come. While photothermal energy has been utilized for centuries by using solar light to heat water and other materials, photovoltaics (PV) provides a means to incorporate directly the produced electrical energy into most of our current infrastructures. After the discovery of the PV effect in the 19th century by Edmond Becquerel [5], it took about 100 years before PVs was used for powering not only small electronic devices, but also space stations and satellites.

Considering the abundance of solar light, one of the "greenest" ways for driving modern science and engineering is to use photochemistry. Solar energy offers the greatest opportunity to harvest the energy over any other renewable energy. With advancing light-harvesting research, solar energy can replace coal and fossil fuels entirely [6].

The events in the recent decades have given a bad reputation to atmospheric CO_2. Nevertheless, in abundance of about 200 ppm, CO_2 is vital for maintaining the climate in which human civilizations flourished. The lack of green-house gases in the atmosphere is as bad as having too much of them. Depleting the carbon dioxide from the atmosphere increases the rates of planetary heat loss and will turn Earth into an ice block [7–9].

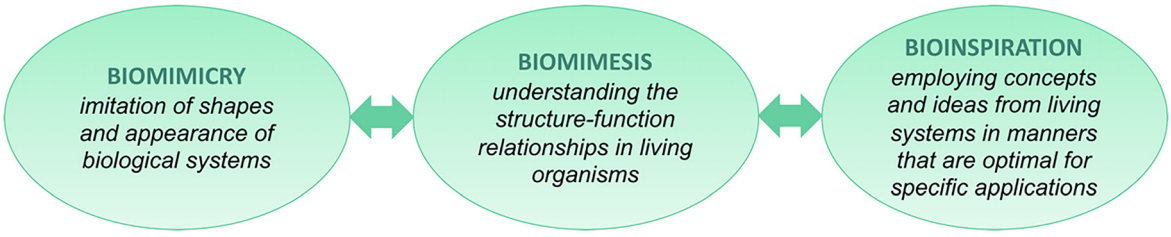

Fig. 1: Evolution of biomimetic to bioinspired approaches.

Atmospheric carbon dioxide also is crucially important for sustaining life on Earth and solar energy makes it possible. By reducing CO_2 to carbohydrates, photosynthesis stores light energy in the form of biological fuels. Biological respiration provides the vital energy for living organisms by "burning" these fuels and releasing CO_2 back in the atmosphere. Therefore, CO_2 is a key part of the shuttling that brings the energy from the photosynthetic sites to all organisms in the biosphere. Fossil fuels represent photosynthetically stored energy in the form of reduced carbon [10]. Humans have developed and perfected technologies for releasing this stored energy, along with CO_2, from fossil fuels. Unfortunately, no technology exists for taking carbon dioxide from the atmosphere and reducing it to store energy. Such a bioinspired solar-fuel industry will be most beneficial not only for human civilization, but also for the planet.

Herein, we introduce the evolution from biomimetic concepts to bioinspired approaches (Fig. 1). To illustrate their impacts, we focus on solar-energy science and engineering.

Biomimicry, biomimetics and bioinspiration

Biomimicry

Biomimicry involves imitation of shapes and appearance of biological systems (Fig. 1) [11]. The amazing diversity of natural occurrences in living organisms, which took millions of years to evolve, have greatly fascinated humans since the down of mankind. Animals and plants have been intricate components of art ever since the Cognitive Revolution (about 70,000 BCE). Agricultural Revolution (about 10,000 BCE) drove the human unification and the rise of civilizations (starting with Sumer about 4,000 BCE), which provided avant-garde tools and immense resources for people to express their observations and imagination. Elements of the flora and the fauna became a part of everyday life. For example, the colonnade motifs of ancient Greece have been the backbone of European and world architecture for centuries. The straightforward Doric order from the western (mainland) Greece, along with its cotemporary Ionic order adopting thin-looking tall shapes from the eastern regions, shaped the images of this ancient civilization. It was the Corinthian order, however, with its characteristic acanthus leaves and other plant and flower motifs at the capitals of the columns that brought the aesthetics of architecture to a completely new level. In his writings from 30 BCE, the Roman architect Vitruvius ascribes the origin of Corinthian style to an Athenian sculptor Callimachus who was inspired by the shapes of tree branches grown through a hanging basket over the grave of a young maiden from Corinth. As a corollary, in the 5^{th} century BCE, Callimachus merged the strengths of the Doric and Ionic orders with biomimicry to create one of the most elegant and beautiful styles of architecture in the ancient world.

While it is common to ascribe the emergence of biomimicry to human ingenuity of mankind, the tendencies for imitating shapes and colors of living organism are not limited to *Homo sapiens*. In order to deter predators, in Batesian mimicry, a benign organism adopts the colors of another organism that is dangerous and threatening. Batesian mimicry in a sense takes advantage of Müllerian mimicry, in which several poisonous, venomous, or foul-tasting organisms imitate from one another patterns of vibrant colors to display distinct warnings to common predators [12]. On the other side of the spectrum, blending with the environment, i.e., camouflage, drastically improves the chances of animals to survive. Camouflage mimicking colored patterns and odors not only keeps vulnerable species hidden from potential predators in their ecosystems, but also provides predators with capabilities to remain undetected as they approach potential prey. Animals, such as moths, octopi, sharks, tigers, chameleons, and many others, illustrate countless examples of importance of camouflage for their survival. For millennia, humans have adopted the biomimicry of camouflage for hunting and military tactics, and overall, for gaining favorable advantages in a wide range of compromising situations.

Biomimesis

Biomimesis represents the next level of adopting the lessons from nature by understanding the structure-function relationships in living organisms (Fig. 1) [11]. Since the commencement of the Scientific Revolution about 500 years ago, following the flourishment of Renaissance, the strives for deep understanding how things truly function have sent the humanity on an exponential trajectory of developments leading to the Industrial Revolution and the Anthropocene. Despite his perfect biomimicry of bird wings, Leonardo da Vinci could not help humans take flight. About a century later, it took Hezârfen Ahmed Çelebi deep understanding of structure-function relationships to be able to take numerous gliding flights from Europe to Asia over the Bosporus. Understanding the effects of the ratios between the wing area and bird weight helped Çelebi succeed where others had failed before him.

The multiscale complexity of structure-function relationships in living organisms leads to emergence of unique properties. Beavers are semiaquatic warm-blooded animals that do not possess thick blubbers, i.e., insulating adipose tissue under their skin, to keep them warm. Nevertheless, they survive in freezing water. The mesoscale structures of their fur, with hydrophobic surfaces, dynamically lock small pockets of air that serve as heat insulators. An international research team from the Massachusetts Institute of Technology and École Polytechnique studied this structure-function relationship and built biomimetics comprising pilli of polydimethylsiloxane that manifest the functionality of the natural systems. The pilli with hydrophobic surface of the artificial systems efficiently trap air [13]. The practicality of advanced "beaver-inspired" diving suits is indisputable. This discovery, however, illustrate the broad scientific impacts of biomimesis. Imitating biological structures allow us to test how well we understand the parameters responsible for their functionality. That is, biomimesis deepens our understanding of how natural systems work.

Bioinspiration

Bioinspiration involves employing concepts and ideas from living systems in manners that are optimal for specific applications (Fig. 1) [11, 14]. Bioinspired structures do not need to resemble their natural counterparts. Most robots, which replaced human labor, do not look like two-legged humanoids. Millions of years of divergent and convergent evolution have produced an amazing variety of organisms with multiscale complexity of perfectly tuned structures and functionalities. Most biological structures become less than useless when taken out of the living organisms. Globular proteins are susceptible to denaturation and self-assembled structures – to degradation. Even if photosynthetic reaction centers within the whole assemblies of thylakoid membranes are wired to electrode surfaces, solar cells containing such biological structures will not operate for long. The lack of self-repairing in manmade devices sets requirements for photostability and durability that is beyond what photosynthetic protein assemblies can offer.

Bioinspiration represents the top level of employing our understanding of living systems for advancing engineering and developing technologies. An impressive but less known example involves the use of a countercurrent multiplier for bioinspired separation of CO_2 and O_2 from other gases. Deepsea fish utilize countercurrent amplification for attaining neutral buoyancy by increasing the partial pressure of O_2 in their swim bladders. It involves loops of blood vessels where oxygen can diffuse from the blood exiting the loops into the blood entering the loops. As oxygenated blood enters such capillary loops, situated around the bladder, a change in pH triggers hemoglobin to release O_2 around the midpoints of the paths along these loops. Some of the freed oxygen diffuses into the bladder, but much of it diffuses into the incoming oxygenated blood flow in the neighboring capillary. That is, the oxygenated blood gets further saturated with O_2 prior to reaching oxygen-release triggering point. This countercurrent amplification results in four orders of magnitude increase in the concertation of oxygen in the swim bladder. Bioinspired microfluidic devices, employing the same countercurrent amplification principles with thermal and photothermal release triggering, demonstrate 2.4-fold enrichment of gas mixtures with CO_2 [15]. The impact of such a bioinspired approach fills a key void in

the solar-fuel engineering. Electrotechnical and photoelectrochemical reduction of CO_2 is achievable. Nevertheless, capturing the diluted atmospheric CO_2 to bring it to the reducing catalytic sites at feasible concentrations is still a formidable challenge.

Striving for artificial photosynthesis

Photosynthetic organisms have produced their food by converting solar energy into chemical one for over two billion years. The amounts of this stored chemical energy drastically exceed what plants and other photosynthetic organisms need for their survival and have driven the flourishment not only of the flora but also of the fauna on our planet. With the discovery of fire and burning wood, humans have mastered the release of this stored energy not only for food, but also for other essentials for survival. The development of social orders employed the fire for a wide range of technological developments that drove the rise of civilizations. The demands of the Industrial Revolution drove the exploration of fossil fuels and mastering the fast release of solar energy deeply stored in the form of reduced carbon. The current marvels of our civilization demand energy at rates surpassing those of capturing the solar energy by the photosynthetic organisms. Humans have perfected the technologies for releasing energy from reduced carbon for millennia. Unfortunately, the balancing act of using sunlight to reduce atmospheric CO_2 is still in the realm of proof-of-principle demonstrations. Artificial photosynthesis has the incomparable potentials to provide the missing link in the energy flow needed for sustaining humanity the way we know it.

Biomimetic molecular systems

In living systems, proteins efficiently mediate electron transfer (ET) and hole transfer (HT) via superexchange mechanism. In the photosynthetic reaction centers, electron hops along porphyrin cofactors arranges in arrays along bundles of transmembrane helices. Therefore, biomimetics composed of synthetic polypeptide helices or of porphyrins have served as important learning tools for deepening the understanding of biological charge transfer (CT) [16–38].

Porphyrin arrays templated in four-helix bundles provide important design principles of polypeptide sequences for achieving desired secondary and tertiary structures [17, 22, 39]. These biomimicry maquettes did not really have the CT functionality of their biological counterparts. For achieving biomimesis, it took resorting to an alternative, non-porphyrin, cofactor with different redox properties to demonstrate efficient long-range CT along such helix bundles [40].

The Pathway Model for CT though biomolecules predict the importance of hydrogen bonds along the CT pathways. The role of hydrogen bonds in the electronic-coupling pathways is still debated because of the complexity of the analysis of experimentally measured rate constants for CT in large protein systems. Relatively simple structures, such as polypeptide helix dimers or short oligopeptides with well-defined conformations, provide an incomparable means to investigate the role of hydrogen bonding on electron-transfer and hole-transfer kinetics [31, 41]. Through-space electronic coupling is even more challenging to characterize than hydrogen-bonding pathways. Biomimetics polypeptide helix dimers mediating CT across leucine zippers reveal the importance of van der Waals contacts in CT pathways [24].

In addition to ET and HT, transmembrane proton “pumping” is a concerted process for energy-conversion biological systems. Reduced quinones are strong Lewis bases. In bacterial photosynthetic reaction centers and in PSII, the long-range electron-transfer along the cofactor doubly reduces plastoquinones, which extract protons from the aqueous media. The formed hydroquinones diffuse across the membranes to get reoxidized and release the protons. Synthetic CT triads and quinones, incorporated in lipid bilayers of liposomes reproduce the functionality of photo-driven proton pumps [42, 43]. Modifying the quinone “shuttle” can introduce a high affinity for chelating Ca^{2+} ions upon reduction. Incorporating such “shuttles” transforms the biomimetic proton pumps into bioinspired light-driven pumps for calcium ions [44]. Charge transfer is

essential for making photosynthesis possible. Its importance reflects the enormous amount of work focused on biomimetic CT systems. Another crucial aspect of PSI and PSII encompasses the catalytic transformations that utilize the photogenerated electrons and holes.

Biomimetic water oxidation to O_2

The generation of molecular oxygen during water oxidation in the PSII involves the extraction of four electrons and protons in four PCET steps at the Mn_4CaO_5 cluster ($2H_2O \rightarrow 4e^- + 4H^+ + O_2$, $E^{(0)} = 1.23$ V vs. NHE). Stepwise oxidation of the Mn centers in the Mn_4CaO_5 cluster, accompanied by PCET, enables the accumulation of four redox equivalents while overcoming high-energy intermediates during the multielectron process. The PCET from the Mn-cluster key for extracting electrons and protons from water to produce oxygen at high rates for hundreds of thousands of cycles [45].

Inspiration from natural principles drives ongoing efforts to design artificial photosynthetic systems for water splitting by employing noble metal complexes, organometallics and inorganic metal oxides as catalysts [46]. Among them, the most popular are based on complexes of manganese, ruthenium, iridium, cobalt and iron [46]. The Mn_4CaO_5 cluster in PCII is ideal for catalyzing water oxidation. The formidable difficulties to construct such heterogeneous catalyst drove the development of a number of its analogues [46, 47]. The performance of these biomimetic structures, however, is unsatisfactory. For example, Brudvig and co-workers reported di-tetrapyridine dimanganese complex that catalyzes water oxidation. This Mn-dimer catalyst is unstable and manifests low activity [48, 49]. After years of improving manganese-based systems, Feng group reported straightforward synthesis of a two-dimensional biomimetic Ca–Mn–O catalyst. This catalyst exhibits excellent activity (TOF = 3.4 s^{-1}) and stability [50]. Conversely, complexes of different metals, such as ruthenium, show decent activity for water oxidation. Developed by Meyer group in the early 1980s, a *bis*-ruthenium bipyridine complex, *cis*,*cis*-$[(bpy)_2(H_2O)Ru^{III}ORu^{III}(H_2O)(bpy)_2]^{4+}$, also known as the *blue dimer*, is the first genuine synthetic catalyst for homogeneous water oxidation [51–55]. Since its first demonstration, researchers have reported a number of its analogues that achieve high TOFs and TONs for water oxidation [56–58]. The success with the ruthenium complexes motivated the expansion of the search for water-oxidation catalysts to chelates of other metal ions from the iron-platinum group, i.e., VIIIB group of the periodic table. Iridium complexes proved to be the third most important group of catalysts for efficient water oxidation [59–61]. As important as the ruthenium and iridium catalysts are for artificial photosynthesis and energy science, however, the scarcity of these elements in the Earth's crust renders them unfeasible for large-scale broad applications.

Biomimetic water reduction to H_2

During photosynthesis, the high-energy electrons extracted from water during the photochemical process, allow for the low-potential reductive chemistry required for fuel production. From a thermodynamic point of view, hydrogen evolution is approximately an equivalent to other important biochemical half reactions involved in fuel productions, such as reduction of $NADP^+$ and CO_2. Relatively easy to produce, H_2 is a candidate for a fuel for storing energy from intermittent carbon-neutral sources, warranting the urgent need for the new catalysts.

Water reduction to H_2 require a strong reductant and redox catalysts to reduce protons to H_2 ($2H^+ + 2e^- \rightarrow H_2$, $E^{(0)} = 0.00$ V vs. NHE). Although this standard electrochemical potential appears quite attainable, the strong dependence of this process on the proton activity, makes water reduction under non-acidic conditions formidably challenging. Biological systems provide an excellent solution for this challenge. Hydrogenases and nitrogenases are immensely effective biocatalysts for generating hydrogen. Engineered protein complexes of hydrogenases and photosynthetic reaction centers provide a bioinspired demonstrations of separating light harvesting from the catalytic sites [62]. Taking this biomimesis further, led to functional systems for water reduction comprising the natural PSI and molecular catalysts [63, 64]. The active sites of the [FeFe], [NiFe] and [Fe] hydrogenases have provide key paradigms in the search of catalysts for

water reduction [65–67]. Going beyond hydrogenases, the Noskov group reported inorganic analogue for nitrogenases – MoS_2 nanoparticles supported on carbon. Their catalyst proved efficient in both electrochemical and photocatalytical hydrogen evolution [68].

A popular, relatively simple, and widely used approach for hydrogen evolution encompasses the use of a one-electron redox reagent, such as methyl viologen (4,4′-dimethyl-bipyridinium, MV^{2+}) as a key intermediate. MV^{2+} is soluble in water and has a reduction potential slightly more negative than that of water ($E^0 = -0.44$ V vs. NHE). Suitable redox catalysts can drive the reoxidation of the reduced form of MV^{2+} with concomitant evolution of H_2 ($MV^{2+} + e^- \rightarrow MV^{\bullet+}$; $2MV^{\bullet+} + 2H^+ \rightarrow 2MV^{2+} + H^2$) [69].

So far, the most effective catalysts for hydrogen evolution from water reduction are based on noble metals. A biomimetic complex of PSI with platinum nanoparticles manifest vigorous light-driven evolution of H_2 [70]. Pt complexes efficiently catalyze electrochemical reduction of water and chelates of Ru and Ir are good choices for driving photoelectrochemical production of H_2. For hydrogen fuel to be a viable alternative, however, its production must be sustainable, rendering the use of scarce and expensive metal complexes unfeasible. In biomimetic systems, enzymes offer key paradigms not only for water reduction under neutral pH, but also for catalytically active site containing only Earth-abundant metals, such as Fe, Ni, and Mo. Biomimetic and bioinspired approaches expand the selection of metals for water-reduction catalysts feasible for large-scale applications [71–75].

Biomimetic water oxidation and reduction processes, leading to oxygen and hydrogen evolution, respectively, demonstrate important features of the catalytic sites that are essential for the development of materials and devices for energy storage in the form of solar fuels.

Bioinspired devices

Most of the key processes in photosynthesis occur in membrane-immobilized proteins or at the interfaces between these structures and the surrounding liquid environment. It is not a surprise, therefore, that liquid-

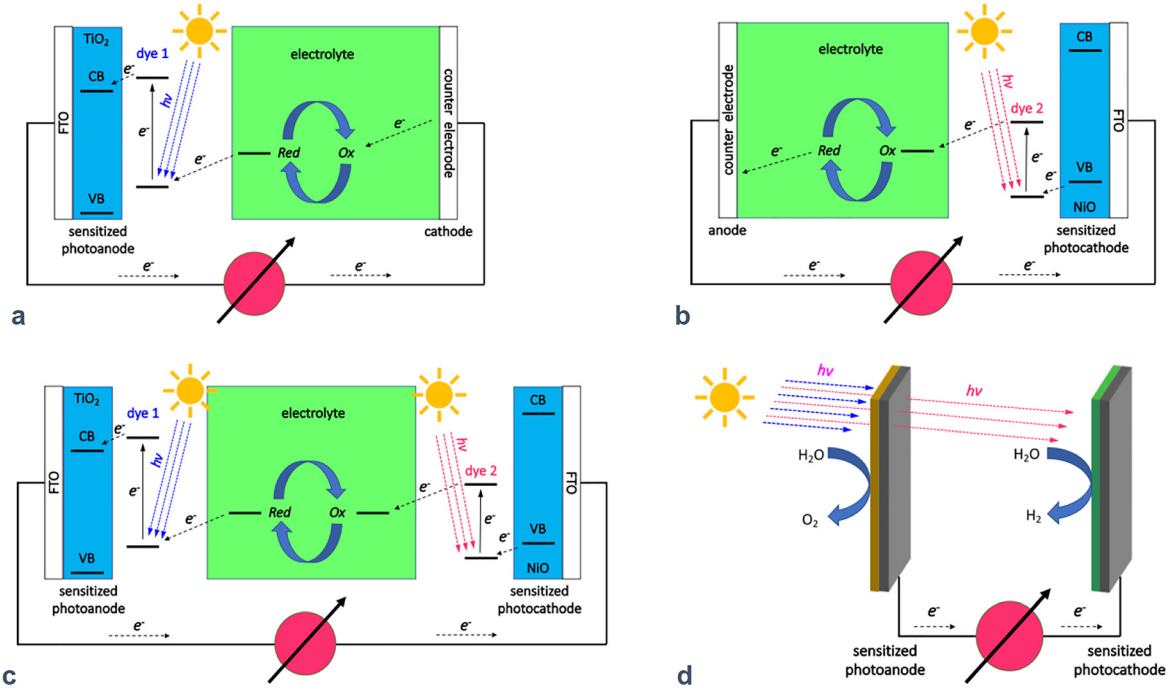

Fig. 2: Evolution of dye sensitized solar cells (DSSCs) toward bioinspired devices for artificial photosynthesis. (a) *n*-DSSC; (b) *p*-DSSC; (c) tandem, *np*-DSSC; and (d) tandem solar cell for photocatalytic splitting of water where the oxidation and the reduction of the redox couple, Ox ⇄ Red, is replaced by chemical transformation for energy storage in the form of H_2 and a release of an oxidant, O_2, in the atmosphere.

junction architectures provide the foundation for transforming the knowledge gained from biomimicry and biomimesis into bioinspired energy engineering (Fig. 2).

Classical (*n*-type) dye sensitized solar cells

The conversion of light into electricity dates back to 1839 when Becquerel discovered that when placing two platinum electrodes into metal halide solution led to the generation of electricity when light is shined on the solution [5, 76]. More than a century later, in the 1960s the discovery that organic dyes possess the capability to convert photons into an electrical current via photoinduced electron transfer from chlorophyll and a ZnO electrode [77–80]. The sensitized ZnO was not truly porous and only absorbed 1 % of sunlight. The research of Brian O'Regan and Michael Grätzel at the end of the 20th century revolutionized this concept of a dye-sensitized solar cell (DSSC) by replacing the ZnO electrode with nanostructured TiO_2, which is also an *n*-type semiconductor (Fig. 2(a)) [81]. Also, replacing the chlorophyll with a photostable ruthenium dyes that have a broad absorption throughout the visible spectral region has drastically improved of the power-conversion efficiencies (η). By 1997, Grätzel achieved DSSCs with η amounting to 10 %, and since then the technology has only improved [82–84].

The biomimesis of using chlorophyll in the first DSSCs achieved photoinduced charge separation and electron transfer (ET) away from the principal chromophore. This demonstration ignited the bioinspired exploration of different dyes and semiconducting materials for achieving the performance we witness today. Shifting the initial choice of chlorophyll sensitizers to metalloorganic dyes made DSSCs viable devices of practical importance. Nevertheless, recent discoveries report some of the highest efficiencies for devices employing porphyrin dye sensitizers [85–88].

In plants and other photosynthetic organisms, the harvested energy from the sunlight converts CO_2 into G3P and eventually into starch or sucrose. Conversely, DSSCs convert solar energy into electricity. In the "classical," i.e., *n*-type, dye-sensitized solar cells (*n*-DSSC), sunlight excites the photosensitizer from its ground to its electronically excited state, which makes it a potent reductant. The conduction band of the *n*-type electrode lies lower than the electron natural transition orbital (NTO) of the excited state of the dye. It allows the passage of the electrons from the photoexcited sensitizer to the working electrode. Under the light-generated electromotive force, the electrons pass through an external circuit to the counter electrode. Inside the cell, a redox shuttle brings them through the liquid electrolyte to the oxidized dye to complete the circuit. The photoanode is the most important component of *n*-DSSCs. Photoanodes mediate not only fast electron transport to prevent charge recombination, but also high charge-separation efficiency with the photosensitizer to ensure close-to-quantitative photocurrent quantum yields [89].

The operation of *n*-DSSCs resembles the functionality of photosystem II (PSII) where the hole on the principal chromophore, after the photoinitiation of the electron-transfer cascade, oxidizes the sacrificial electron donor – water – to release molecular oxygen. The cathode is a passive source of holes for the external circuit, instead of providing extra photoreducing power like photosystem I (PSI). The quest for such key complementary component, missing from the classical DSSCs, drove the development of *p*-type dye sensitized solar cells (*p*-DSSCs) where a photocathode provides the electromotive force.

Inverted (*p*-type) dye sensitized solar cells for completing the circuit

The inverted DSSCs (i.e., *p*-DSSCs), have similar operational principles as the *n*-DSSCs, but mediate photodriven currents in the opposing direction, as the name suggests (Fig. 2(b)) [90, 91]. Instead of sensitized photoanode of *n*-type semiconducting oxide, such as TiO_2, ZnO and SnO_2, *p*-DSSC possess photocathodes of *p*-semiconductors, such as NiO, Cu_2O, $CuGaO_2$ and $CuAlO_2$, that are sensitized with electron deficient dyes [92–104]. The hole NTO of the photoexcited sensitizer lies below the valence band edge of the *p*-semiconductor, allowing for photoinduced hole injection in the cathode. The holes pass through the external circuit, and redox shuttles bring them to the photoreduced dye to reoxidize it. The amount of research on *p*-DSSCs has been miniscule in comparison with the research and development efforts on *n*-DSSCs. It is not a surprise that

currently *p*-DSSCs perform considerably less efficiently than the *n*-type devices. The dire need for functional photocathodes in the pursuit of artificial photosynthesis and solar fuels drives the search for electron-deficient dyes, redox shuttles and *p*-type materials need to make *p*-DSSCs a viable energy technology [102, 105].

Neither *p*-DSSCs, nor *n*-DSSCs, on their own can drive the progress toward artificial photosynthesis. Ideally, tandem DSSCs with photocathodes and photoanodes absorbing in different regions of the solar spectrum while producing the same photocurrent, is the way to overcome the Shockley–Queisser limit inherent for single-junction devices [106–109]. The tandem operation of PSII and PSI, driving the photochemical splitting of water to O_2 and NADPH, provides excellent paradigms for achieving functional *np*-DSSCs (Fig. 2(c)).

Sold-state devices offer certain advantages for photovoltaics (PVs) [110, 111]. The wide installation of silicon solar panels in commercial and residential properties, and the unprecedentedly fast development of PVs based on halide perovskite materials illustrate the preference for all solid-state solar cells. Nevertheless, liquid-junction devices, such as DSSCs, have unique features that are crucial for the pursuit of artificial photosynthesis (Fig. 2(d)). The liquid-solid interfaces are essential for introducing electrocatalytic and photocatalytic sites. Therefore, liquid-junction devices provide an incomparable platform for bringing the energy engineering beyond the sunlight-driven electricity production. Photoelectrocatalytic devices based on *np*-DSSCs, which store solar energy in the form of easy-to-transport reduced fuels (Fig. 2(d)), while releasing oxygen gas as a side product, can undoubtedly serve as the missing link for sustainable technological growth.

Field effects on charge transfer

Strive for electroneutrality

The inherent strength and the relatively long range of electric forces make ET and HT immensely susceptible to surrounding charged and dipolar species. For estimating CT driving forces, $-\Delta G_{CT}^{(0)}$, the Coulombic and Born-solvation terms in the Rehm-Weller equation account for these electrostatic interactions [112, 113]:

$$\Delta G_{CT^{(0)}} = F\left(E_{D^{\cdot+}|D} - E_{A|A^{\cdot-}}\right) - \mathcal{E}_{00} + \Delta G_S + W \tag{1}$$

Where $E_{D^{\cdot+}|D}$ is the reduction potential of the oxidized donor and $E_{A|A^{\cdot-}}$ is the reduction potential of the acceptor; F is the Faraday constant; and $\mathcal{E}_{00}$ is the zero-to-zero energy, i.e., optical excitation energy, of the donor (for photoinduced electron transfer, $\Delta G_{ET}^{(0)}$), and of the acceptor (for photoinduced hole transfer, $\Delta G_{HT}^{(0)}$) [114]. The Coulombic term, W, quantifies the interactions between donor and the acceptor [113, 115]. The Born-solvation term, ΔG_S, on the other hand, accounts for the interactions of the donor and the acceptor with the medium environment by correcting their reduction potentials [113, 116]. (Eq. (1) is not to be confused with the empirical expression, also called Rehm-Weller equation, for the driving-force dependence of CT rates for cases that do not show the Marcus inverted region [112, 114]).

Transferring an electron from a donor to an acceptor changes the electric-field profiles around them and induces rearrangements of dipoles and ions in the surrounding environment, as accounted by the medium, i.e., outer-sphere, reorganization energy [117–119]. In attempts to maintain electroneutrality, dipoles reorient and counterions move around. In solid media, lattice deformations around electrons and holes induce similar polarization to stabilize the transferred charges, forming polarons [120–125].

As aliphatic amides, peptide bonds are some of the most polar groups in biomolecules [126], which warrants sizable reorganization energies for CT in proteins. In fact, polaron models can describe ET and HT in globular proteins [127].

When the medium can reorganize faster than charge transfer, a static description of the initial and final states based on the Born solvation energy using the inverse dielectric constants of the environment, i.e., ε^{-1} and n^{-2}, depicts well the features of the CT kinetics [114, 128]. When CT is faster than medium reorganization, on the other hand, the rearrangement of the solvent molecules and the counter ions becomes the rate-limiting step

and not only can drastically slow down the transfer of electrons and holes, but also alter the preferred mechanism especially when multiple parallel pathways are in operation [129–131].

An increase in medium viscosity to a point of reaching a solid state grossly limits the rotation of the solvent molecules for reorienting their permanent dipoles and the movement of ions around the solvation cavity. A static description of the initial and final states can quantify the CT kinetics of such "frozen" systems. Indeed, solidifying polar solvents that favor CT states drastically lowers their static dielectric constants because of suppression of orientational (dipolar) polarization, i.e., $\varepsilon \to n^2 + \varepsilon_v$, where ε_v is the contribution to the dielectric constant originating from the nuclear polarization. At low temperatures, for example, the static dielectric constant of ice, i.e., frozen water, is comparable to that of a non-polar solvents. Upon transitioning from 15 to –185 °C, ε of water drops from 80 to about 2.4–2.9, of glycerol (which is a viscous solvent at room temperature) – from 56 to 3.2, of nitrobenzene – from 32 to 2.6, and of ethanol – from 25 to 3.1 [132].

Even with a knowledge about the bulk dielectric properties of solid solvents, the broadly used static treatments of the initial and final states often assume continuous homogeneous polarization around donor and the acceptor. They do not account for discrete molecular ordered arrangements of dipoles and counterions in relevance to the donor and the acceptor. Effects of such permanently oriented electric dipoles can be enormous and they are the focus of the next section.

Movement of anions along with HT, and of cations with ET, allows for concerting electroneutrality. Therefore, the migration of the counterions of systems with positively charged acceptors or negatively charged donors can be deterministic for the rates of HT or ET, which involves charge shifts [133, 134]. Placing such systems in a solid medium, which suppresses the ion migration, drastically alters the CT kinetics [135].

Proton-coupled electron transfer (PCET) is one of the most important process in biology where co-directional transduction of an electron and a cation concerts electroneutrality [136–138]. PCET is especially important for the interior of globular proteins where protons are the most abundant candidate for labile cations for concerting electroneutrality during ET. In PSII, tyrosine-Z, i.e., D1Tyr161 (Y_Z), is crucial for the HT from the oxidized P680 special pair to the water-oxidizing Mn–Ca complex. Proton transfer aids the transduction of electrons toward $P680^{\bullet+}$. This PCET has been the focus of extensive mechanistic studies; and YZ with its hydrogen-bonding motif has served as a key paradigm for biomimetic and bioinspired structures with advanced CT properties [139–143].

Effects of permanent electric dipoles on charge transfer

Electric dipoles generate localized fields that can reach GV m^{-1} in their proximity, but rapidly fall off with distance, especially in polar media. For non-polar solvents, therefore, the effects of permanently oriented dipoles on CT are enormous when they are located near the donors and acceptors or incorporated in one of them [144, 145]. Protein interior, comprising a huge number of polar groups, such as the amides of the backbones, in a relatively non-polar surrounding of mostly aliphatic chains, represents the situation where dipole-generated fields form complex networks of potentials that can govern CT. Such biomolecular systems triggered the interest in dipole effects on CT in the mid-20th century [146, 147].

The accepted notion for dipole effects on CT focusses on the driving force. The potentials from the dipole-generated fields exerted on the donor and the acceptor, i.e., $\phi_{\boldsymbol{\mu}^{(D)}}$ and $\phi_{\boldsymbol{\mu}^{(A)}}$, respectively, modulate their reduction potentials and the overall the CT driving force [114, 144]:

$$\Delta G_{CT^{(0)}} = F\left(\left(E_{D^{\bullet+}|D} + \phi_{\boldsymbol{\mu}^{(D)}} \right) - \left(E_{A|A^{\bullet-}} + \phi_{\boldsymbol{\mu}^{(A)}} \right) \right) - \mathcal{E}_{00} + \Delta G_S + W \tag{2}$$

When CT affects the dipoles generating the external potentials, it is important to consider this change in $\phi_{\boldsymbol{\mu}}$ and how it affects the reduction potentials, as we showed in the quantification of these effects using Eq. (2) [144].

In living systems, dipole effects on CT and ion transport are vital [148–150]. The complexity of such systems, however, warrants challenging analysis to relate the observed CT kinetics with the dipolar structural

features. Therefore, biomimetic electrets emerged as principal tool for furthering the field. With ordered electric dipole moments, electrets are the electrostatic analogues of magnets.

Biomimetic molecular electrets

While the ideas for dipole effects on CT emerged in the 1960s, it was the 1990s when Galoppini and Fox demonstrated experimentally dipole-induced rectification of long-range CT employing polypeptide helices as macromolecular electrets [21, 25, 26]. Using a polypeptide as a bridge in donor-bridge-acceptor systems, the analysis revealed that CT is much faster when electrons move along the dipole rather than against it [21].

Protein helices are some of the best molecular electrets. For example, α-helices have permanent dipole moments oriented from their N- to their C-termini (Fig. 3), originating from the codirectional hydrogen-bonding polarization and the ordered amides on the backbone, and amounting to about 5 Debyes per residue [148, 151]. The 3_{10}-helices are more tightly strained than the α-helices. As the name suggests, these conformers contain three residues per turn and 10-bond loops between neighboring hydrogen bonds that hold the structure together. Following this nomenclature, α-helices are in fact 3.6_{13}-helices [152]. Each residue contributes about 4.6 Debyes to the overall dipole moment of 3_{10}-helices [151]. While α-helices have slightly larger macrodipoles than the 3_{10} conformers, the tight 3_{10}-helix structures are more stable folds than the α-helices for short polypeptides, i.e., shorter than 20 amino-acid residues. On the other side of the spectrum, with 4.1 residues per turn, π-helices are more loosely folded than α-helices [153–155]. Despite their abundance in nature, π-helices predominantly exist as single-loop folds of short segments of about seven residues.

Containing only tertiary amides along their backbones, polyproline (PP) assumes helical conformations without hydrogen bonding networks. Therefore, the PP macrodipoles originate only from the ordered amides and are smaller than those of the other protein helices [151]. The different conformations of the peptide bonds results in two types of PP helices: polyproline I (PPI) and polyproline II (PPII). In PPI helices, the backbone amides assume *Z* conformation with their dipole orientated from the N- to C-termini, contributing about 4.1 D per residue to the macrodipole [151]. The PPII helices contain E-conformers of the amides resulting in macrodipoles of about 1.5 D (or less) per residue, oriented from their C- to their N-termini [151], i.e., in same direction as that of the α-helix and 3_{10}-helix dipoles (Fig. 3). A change in solvent polarity induces a switch between PPI and PPII conformations. The amide bond planes of PPII are near orthogonal to the principal helix axis. Therefore, relatively small structural changes, often induced by the solvent media, induce sizable variations of the PPII macrodipole from about 0 to 1.5 D per residue.

This wealth of electronic features of polypeptide helices made these structures the preferred choice for biomimetic electrets to unravel the dipole effects on CT in the first decades of the 21st century (ref). The use of polypeptide conformers for CT scaffolds, however, poses some challenging limitations: (1) the conformational integrity of polypeptide α-helices is often compromised when taken out of their natural environment, thus

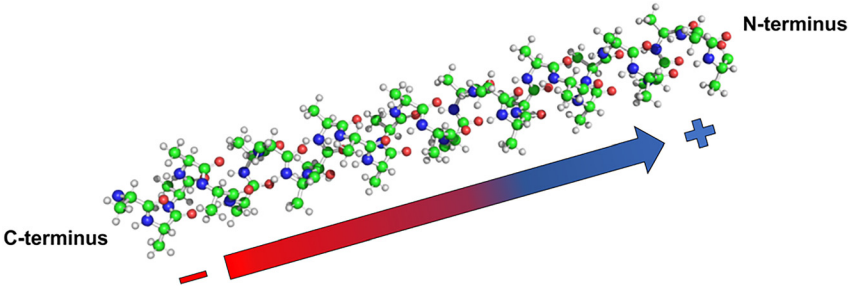

Fig. 3: Balls-and-sticks model of a polypeptide α-helix composed of alanine residues, representing one of the best known molecular electrets as indicated by its permanent electric macrodipole.

limiting the scopes of their applications, and (2) injection of electrons or holes in polypeptides composed of natural α-amino acids leads to their reductive or oxidative degradation, respectively, preventing them from mediating long-range CT via hopping. Along their backbones, therefore, polypeptides mediate CT only via quantum mechanical tunneling, or super-exchange mechanism, the rates of which exponentially decrease with distance. Such rates become unfeasibly small for attaining efficient CT (initiated by excited states with nanosecond lifetimes) at distances exceeding about 2 nm. Conversely, incoherent charge hopping along (1) protein cofactors, (2) redox-active amino-acid side chains, and (3) π-stacked base pairs in polynucleotides, allows biomolecules and their assemblies to efficiently mediate CT at impressively long ranges. These inherent limitations of biomimetic electrets warrant the implementation of bioinspired approaches to further the advances of the field [11, 14].

Bioinspired molecular electrets

While biomimetics play a crucial role in exploratory research and in basic science, their technological implementations are somewhat limited. The translation from basic to applied science and from exploratory to developmental research is where bioinspiration takes over. In addition to driving the scientific discoveries to applied engineering, biological inspirations open unprecedented fields for exploration of new properties and phenomena that cannot emerge from natural systems.

Combining the structural motifs of protein helices, responsible for the intrinsic macrodipoles, with the concepts of biological arrays that mediate long-range CT, we developed bioinspired molecular electrets based on anthranilamide (Aa) structures (Fig. 4) [156–158]. The Aa bioinspired electrets are aromatic oligo-ortho-amides with their extended structures supported by a hydrogen-bond network (Fig. 4). Similar to protein helices, ordered amide and hydrogen bonds generate macrodipoles along the backbones of the Aa oligomers amounting to about 3 D per residue [156, 157]. Unlike proteins and synthetic polypeptide helices, aromatic moieties, directly linked with amide bonds, provide sites for electron or hole hopping that are essential for attaining long-range CT. The electric fields resultant from such ordered dipoles can visibly affect the CT processes they mediate (Eq. (2)). That is, the dipole-generated local electric fields can serve as important tools for accelerating desired CT processes, while suppressing undesired ones [144, 145], which is paramount not only for conversion and storage of harvested solar energy, but also for organic and molecular electronics. Similar to other polypeptides, the chemical synthesis of Aa electret proceeds from their C- to their N-termini. Despite all the advances in peptide chemistry, none of the established synthetic protocols is applicable for the synthesis of Aa oligomers because of key structural differences between anthranilic-acid derivatives and the analogues of the native α-amino acids [159]. Instead of using anthranilic acids with protected β-amines, introducing each residue as the corresponding derivative of the 2-nitrobenozic acid addresses the grave inherent challenges for making polypeptides based on Aa structures [156, 159]. The building of Aa molecular electrets involves a series of amide-coupling and selective nitro-group-reduction steps [156, 159, 160]. Adopting this approach, we have developed robust methodologies for reliable synthesis of Aa oligomers [159, 160].

To determine the extent at which Aa dipoles affect CT, we compare the rates of ET towards the C-termini versus the N-termini of an electron-rich Aa residue, defining CT rectification as $R = \lg (k_{N\rightarrow C}/k_{C\rightarrow N})$ [145]. Specifically, we construct dyads comprising Aa as an electron donor and 1-alkylpyrene (Py) as an electron acceptor (Fig. 5). These donor-acceptor dyads distinctly rectify not only the forward photoinduced ET, but also

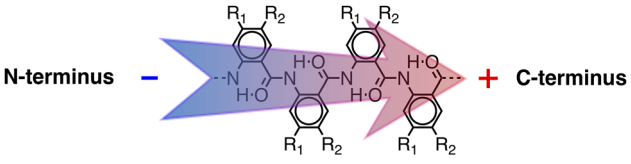

Fig. 4: Bioinspired molecular electret composed of anthranilamide (Aa) residues and its permanent electric dipole moment.

the subsequent CR [145], which was a key step forward in the field of dipole-modulated CT. Our findings show that charge separation (CS) is faster when the electron moves along the dipole than when it moves against it, which perfectly agrees with the accepted notion for the dipole effects on the CT driving forces, $-\Delta G^{(0)}$. The observed rectification of CS decreases with an increase in medium polarity, which is consistent with screening of the dipole-generated localized electric field [145]. The charge-recombination (CR) rates are also larger when the electron moved along the dipole than against it [145]. Because of the large $-\Delta G_{CR}^{(0)}$, CR operates in the Marcus inverted region and the observed dipole effect on CR appears to contradict the transition-state theory. An increase in solvent polarity, however, which screens the dipole field, leads to a slight increase in the CR rectification [145]. These findings indicate that the donor-acceptor electronic-coupling, in addition to the Franck-Condon factors (via the thermodynamic driving forces), govern the CR kinetics [145]. This first demonstration of an interplay between the dipole effect on $\Delta G_{CR}^{(0)}$ and the donor-acceptor electronic coupling illustrates the power of biological inspiration for the discovery of new emerging properties and phenomena.

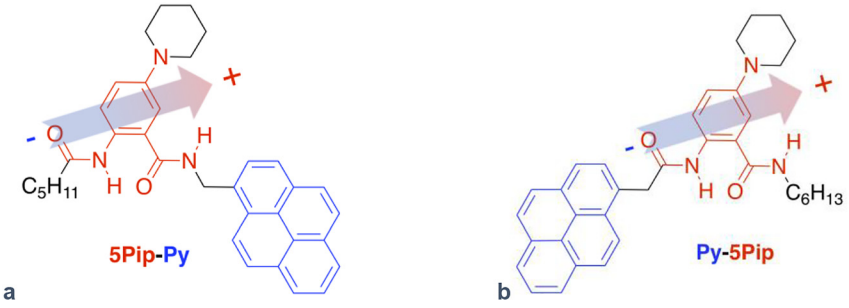

Fig. 5: Donor-acceptor dyads composed of an electron-rich Aa residue (**5Pip**) as a donor and pyrene (**Py**) as an acceptor. The Aa residue also bears a permanent electric dipole moment of about 6 D. (a) **5Pip-Py** that mediates photoinduced CS involving ET along the dipole and CR – ET against the dipole. (a) **Py-5Pip** that mediates photoinduced CS involving ET against the dipole and CR – ET along the Aa dipole.

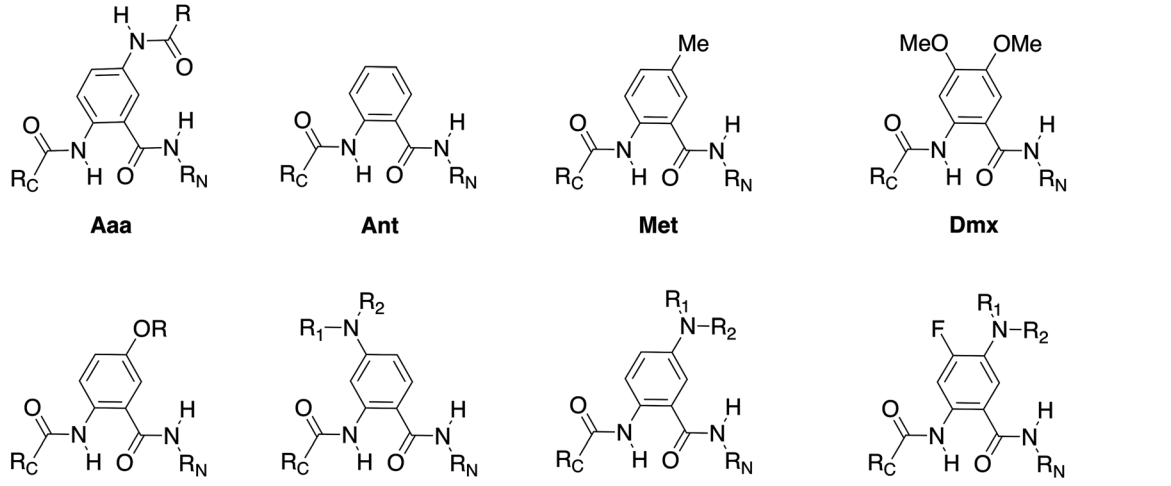

Fig. 6: Anthranilamide (Aa) residues with electron-donating side chains (R_1 and R_2, Fig. 4) for building hole-transfer (*p*-type) bioinspired molecular electrets.

These immensely encouraging results set the foundation for developing a broad variety of Aa residues with diverse electronic and optical features (Fig. 6).

Each of the Aa residues can have two side chains (R_1 and R_2, Fig. 4). These side chains are essential for controlling the solubility and aggregation propensities of the Aa structures [161]. In addition, varying the Aa side chains provides an important handle for modifying the electronic and optical properties of these conjugates [162–165]. That is, a library of Aa residues with different R_1 and R_2 represents a synthetic proteome for structures with countless electronic and photonic functionalities [14, 163, 166]. Our initial focus has been on hole-transfer Aa residues with electron-donating side chains. Varying the electron-donating strength of the R_1 and R_2 groups from amines to alkyls, adjusts the reduction potentials of Aa oxidation over a range of 1 V [161–164]. For pursuing CT via hole hopping mechanism, it is essential for the oxidized residues, $Aa^{\bullet+}$, to manifest reasonable stability [162, 167]. Aliphatic and aromatic amides have notorious propensity for degradation when oxidized at potentials exceeding about 1.4–1.5 V vs. SCE, which is an underlying reason why proteins cannot sustainably mediate hole hopping along their backbones. Recently, we discovered that using ether substituents for R_2 can stabilize the $Aa^{\bullet+}$ oxidized species at potentials exceeding 1.5 V vs. SCE (Box, Hox, Fox and Dmx, Fig. 6), as evident from the reversibility of their electrochemical oxidation [168]. Making Aa oligomers of such residues with ether side chains provides paths toward attaining amide electrets that can transfer strongly oxidizing holes [160]. The diversity of electronic structures that Aa bioinspired molecular electrets offer (Fig. 6), makes them a perfect platform for exploring dipole effects not only on CT, but also on electronic and photonic dynamics at different scales. Local electric fields, originating from molecular dipoles, have profound effects on the electronic properties of the microenvironment. Overall, local electric fields from molecular dipoles affect ET and HT, providing a promising means for increasing the efficiency of the desired CT processes while suppressing the undesired ones.

Conclusions

With their complexity and diversity, living systems offer a wealth of incomparable information that have driven human ingenuity for thousands of years. The shear imitation that biomimicry implements offer the initial steps of understanding biological systems. In the search of functionalities, biomimesis considerably deepens this understanding. Bioinspiration paves the ways for taking this knowledge and implement it in "practical" manners to meet key engineering demands. The impacts of bioinspiration are not limited only to its utilitarian values. Employing biological concepts in abiotic manners, has made bioinspired approaches uniquely powerful for exploring structure-function relationships that do not exist in nature, and at the same time, are uncommon for other the fields of the fundamental sciences.

Research funding: The funding was provided by the USA National Science Foundation, grant CHE 1800602, and by the American Chemical Society, Petroleum Research Fund, grant 60651-ND4.

References

[1] D. Gielen, F. Boshell, D. Saygin, M. D. Bazilian, N. Wagner, R. Gorini. *Energy Strateg. Rev.* **24**, 38 (2019).
[2] P. A. Owusu, S. Asumadu-Sarkodie. *Cogent Eng.* **3**, 1167990 (2016).
[3] A. Demirbas. *Energy Sources Part A* **28**, 779 (2006).
[4] A. Henderson-Sellers, M. F. Wilson. *Phil. Trans. Roy. Soc. Lond.* **309**, 285 (1983).
[5] A.-E. Becquerel. *Compt. Rend.* **9**, 561 (1839).
[6] V. Kumar, R. L. Shrivastava, S. P. Untawale. *Aquat. Pr.* **4**, 473 (2015).
[7] A. A. Lacis, G. A. Schmidt, D. Rind, R. A. Ruedy. *Science* **330**, 356 (2010).
[8] W. Steffen, K. Richardson, J. Rockström, S. E. Cornell, I. Fetzer, E. M. Bennett, R. Biggs, S. R. Carpenter, W. de Vries, C. A. de Wit, C. Folke, D. Gerten, J. Heinke, G. M. Mace, L. M. Persson, V. Ramanathan, B. Reyers, S. Sörlin. *Science* **347** (2015), https://doi.org/10.1126/science.1259855.

[9] A. Indermuhle, T. F. Stocker, F. Joos, H. Fischer, H. J. Smith, M. Wahlen, B. Deck, D. Mastroianni, J. Tschumi, T. Blunier, R. Meyer, B. Stauffer. *Nature* **398**, 121 (1999).
[10] G. Ciamician. *Science* **36**, 385 (1912).
[11] V. I. Vullev, J. Phys. *Chem. Lett.* **2**, 503 (2011).
[12] S. Lev-Yadun. *Plant Signal. Behav.* **13** (2018), https://doi.org/10.1080/15592324.2018.1480846.
[13] A. Nasto, M. Regli, P. T. Brun, J. Alvarado, C. Clanet, A. E. Hosoi. *Phys. Rev. Fluids* **1** (2016), https://doi.org/10.1103/physrevfluids.1.033905.
[14] E. M. Espinoza, J. M. Larsen-Clinton, M. Krzeszewski, N. Darabedian, G. D. T, V. I. Vullev. *Pure Appl. Chem.* **89**, 1777 (2017).
[15] K. Brubaker, A. Garewal, R. C. Steinhardt, A. P. Esser-Kahn. *Nat. Commun.* **9** (2018), https://doi.org/10.1038/s41467-018-03052-y.
[16] V. I. Vullev, G. Jones, II. *Res. Chem. Intermed.* **28**, 795 (2002).
[17] D. E. Robertson, R. S. Farid, C. C. Moser, J. L. Urbauer, S. E. Mulholland, R. Pidikiti, J. D. Lear, A. J. Wand, W. F. DeGrado, P. L. Dutton. *Nature* **368**, 425 (1994).
[18] C. T. Choma, J. D. Lear, M. J. Nelson, P. L. Dutton, D. E. Robertson, W. F. DeGrado. *J. Am. Chem. Soc.* **116**, 856 (1994).
[19] G. Jones, II, L. N. Lu, V. Vullev, D. Gosztola, S. Greenfield, M. Wasielewski. *Bioorg. Med. Chem. Lett.* **5**, 2385 (1995).
[20] F. Rabanal, B. R. Gibney, W. F. DeGrado, C. C. Moser, P. L. Dutton. *Inorg. Chim. Acta.* **243**, 213 (1996).
[21] E. Galoppini, M. A. Fox. *J. Am. Chem. Soc.* **118**, 2299 (1996).
[22] F. Rabanal, W. F. DeGrado, P. L. Dutton. *J. Am. Chem. Soc.* **118**, 473 (1996).
[23] M. W. Mutz, G. L. McLendon, J. F. Wishart, E. R. Gaillard, A. F. Corin. *Proc. Natl. Acad. Sci. U.S.A.* **93**, 9521 (1996).
[24] G. V. Kozlov, M. Y. Ogawa. *J. Am. Chem. Soc.* **119**, 8377 (1997).
[25] M. A. Fox, E. Galoppini. *J. Am. Chem. Soc.* **119**, 5277 (1997).
[26] A. Knorr, E. Galoppini, M. A. Fox. *J. Phys. Org. Chem.* **10**, 484 (1997).
[27] G. Jones, V. Vullev, II, E. H. Braswell, D. Zhu. *J. Am. Chem. Soc.* **122**, 388 (2000).
[28] A. Y. Kornilova, J. F. Wishart, W. Xiao, R. C. Lasey, A. Fedorova, Y.-K. Shin, M. Y. Ogawa. *J. Am. Chem. Soc.* **122**, 7999 (2000).
[29] G. Jones, V. I. Vullev, II. *Org. Lett.* **3**, 2457 (2001).
[30] G. Jones, V. I. Vullev, II. *J. Phys. Chem.* **105**, 6402 (2001).
[31] G. Jones, V. I. Vullev, II. *Org. Lett.* **4**, 4001 (2002).
[32] V. I. Vullev, G. Jones. *Tetrahedron Lett.* **43**, 8611 (2002).
[33] Y. Zheng, M. A. Case, J. F. Wishart, G. L. McLendon. *J. Phys. Chem. B* **107**, 7288 (2003).
[34] G. Jones, X. Zhou, II, V. I. Vullev. *Photochem. Photobiol. Sci.* **2**, 1080 (2003).
[35] M. A. Case, G. L. McLendon. *Accounts Chem. Res.* **37**, 754 (2004).
[36] S. A. Serron, W. S. Aldridge, C. N. Fleming, R. M. Danell, M. H. Baik, M. Sykora, D. M. Dattelbaum, T. J. Meyer. *J. Am. Chem. Soc.* **126**, 14506 (2004).
[37] M. H. V. Huynh, D. M. Dattelbaum, T. J. Meyer. *Coord. Chem. Rev.* **249**, 457 (2005).
[38] Y. Chen, J. Viereck, R. Harmer, S. Rangan, R. A. Bartynski, E. Galoppini. *J. Am. Chem. Soc.* **142**, 3489 (2020).
[39] G. Ghirlanda, A. Osyczka, W. Liu, M. Antolovich, K. M. Smith, P. L. Dutton, A. J. Wand, W. F. DeGrado. *J. Am. Chem. Soc.* **126**, 8141 (2004).
[40] L. Cristian, P. Piotrowiak, R. S. Farid. *J. Am. Chem. Soc.* **125**, 11814 (2003).
[41] R. OrS owski, J. A. Clark, J. B. Derr, E. M. Espinoza, M. F. Mayther, O. Staszewska-Krajewska, J. R. Winkler, H. Ja drzejewska, A. Szumna, H. B. Gray, V. I. Vullev, D. T. Gryko. *Proc. Natl. Acad. Sci. U. S. A.* **118**, e2026462118 (2021).
[42] G. Steinberg-Yfrach, P. A. Liddell, S.-C. Hung, A. L. Moore, D. Gust, T. A. Moore. *Nature* **385**, 239 (1997).
[43] G. Steinberg-Yfrach, J.-L. Rigaud, E. N. Durantini, A. L. Moore, D. Gust, T. A. Moore. *Nature* **392**, 479 (1998).
[44] I. M. Bennett, H. M. V. Farfano, F. Bogani, A. Primak, P. A. Liddell, L. Otero, L. Sereno, J. J. Silber, A. L. Moore, T. A. Moore, D. Gust. *Nature* **420**, 398 (2002).
[45] P. Kurz. in *Solar Energy for Fuels*, H. Tüysüz, C. K. Chan (Eds.), p. 49, Springer International Publishing, Cham (2016).
[46] K. S. Joya, H. J. M. de Groot. *Int. J. Hydrogen Energy* **37**, 8787 (2012).
[47] J. S. Kanady, E. Y. Tsui, M. W. Day, T. Agapie. *Science* **333**, 733 (2011).
[48] J. Limburg, J. S. Vrettos, H. Y. Chen, J. C. de Paula, R. H. Crabtree, G. W. Brudvig. *J. Am. Chem. Soc.* **123**, 423 (2001).
[49] J. Limburg, J. S. Vrettos, L. M. Liable-Sands, A. L. Rheingold, R. H. Crabtree, G. W. Brudvig. *Science* **283**, 1524 (1999).
[50] Z. B. Geng, Y. Sun, Y. Zhang, Y. X. Wang, L. P. Li, K. K. Huang, X. Y. Wang, J. H. Liu, L. Yuan, S. H. Feng. *ACS Appl. Mater. Interfaces* **10**, 37948 (2018).
[51] S. W. Gersten, G. J. Samuels, T. J. Meyer. *J. Am. Chem. Soc.* **104**, 4029 (1982).
[52] J. A. Gilbert, D. S. Eggleston, W. R. Murphy, D. A. Geselowitz, S. W. Gersten, D. J. Hodgson, T. J. Meyer. *J. Am. Chem. Soc.* **107**, 3855 (1985).
[53] J. K. Hurst, J. Z. Zhou, Y. B. Lei. *Inorg. Chem.* **31**, 1010 (1992).
[54] C. W. Chronister, R. A. Binstead, J. F. Ni, T. J. Meyer. *Inorg. Chem.* **36**, 3814 (1997).
[55] F. Liu, J. J. Concepcion, J. W. Jurss, T. Cardolaccia, J. L. Templeton, T. J. Meyer. *Inorg. Chem.* **47**, 1727 (2008).
[56] E. L. Lebeau, S. A. Adeyemi, T. J. Meyer. *Inorg. Chem.* **37**, 6476 (1998).
[57] C. Sens, I. Romero, M. Rodriguez, A. Llobet, T. Parella, J. Benet-Buchholz. *J. Am. Chem. Soc.* **126**, 7798 (2004).

[58] R. Zong, R. P. Thummel. *J. Am. Chem. Soc.* **127**, 12802 (2005).
[59] N. D. McDaniel, F. J. Coughlin, L. L. Tinker, S. Bernhard. *J. Am. Chem. Soc.* **130**, 210 (2008).
[60] J. F. Hull, D. Balcells, J. D. Blakemore, C. D. Incarvito, O. Eisenstein, G. W. Brudvig, R. H. Crabtree. *J. Am. Chem. Soc.* **131**, 8730 (2009).
[61] J. D. Blakemore, N. D. Schley, D. Balcells, J. F. Hull, G. W. Olack, C. D. Incarvito, O. Eisenstein, G. W. Brudvig, R. H. Crabtree. *J. Am. Chem. Soc.* **132**, 16017 (2010).
[62] D. Mersch, C. Y. Lee, J. Z. Zhang, K. Brinkert, J. C. Fontecilla-Camps, A. W. Rutherford, E. Reisner. *J. Am. Chem. Soc.* **137**, 8541 (2015).
[63] L. M. Utschig, S. C. Silver, K. L. Mulfort, D. M. Tiede. *J. Am. Chem. Soc.* **133**, 16334 (2011).
[64] L. M. Utschig, S. R. Soltau, D. M. Tiede. *Curr. Opin. Chem. Biol.* **25**, 1 (2015).
[65] T. R. Simmons, G. Berggren, M. Bacchi, M. Fontecave, V. Artero. *Coord. Chem. Rev.* **270**, 127 (2014).
[66] D. Brazzolotto, M. Gennari, N. Queyriaux, T. R. Simmons, J. Pecaut, S. Demeshko, F. Meyer, M. Orio, V. Artero, C. Duboc. *Nat. Chem.* **8**, 1054 (2016).
[67] M. A. Gross, A. Reynal, J. R. Durrant, E. Reisner. *J. Am. Chem. Soc.* **136**, 356 (2014).
[68] B. Hinnemann, P. G. Moses, J. Bonde, K. P. Jorgensen, J. H. Nielsen, S. Horch, I. Chorkendorff, J. K. Norskov. *J. Am. Chem. Soc.* **127**, 5308 (2005).
[69] S. Fukuzumi. *Eur. J. Inorg. Chem.* **2008**, 1351 (2008).
[70] L. M. Utschig, N. M. Dimitrijevic, O. G. Poluektov, S. D. Chemerisov, K. L. Mulfort, D. M. Tiede. *J. Phys. Chem. Lett.* **2**, 236 (2011).
[71] N. P. Nguyen, B. L. Wadsworth, D. Nishiori, E. A. Reyes Cruz, G. F. Moore. *J. Phys. Chem. Lett.* **12**, 199 (2021).
[72] B. L. Wadsworth, D. Khusnutdinova, J. M. Urbine, A. S. Reyes, G. F. Moore. *ACS Appl. Mater. Interfaces* **12**, 3903 (2020).
[73] B. L. Wadsworth, A. M. Beiler, D. Khusnutdinova, E. A. Reyes Cruz, G. F. Moore. *J. Am. Chem. Soc.* **141**, 15932 (2019).
[74] D. Khusnutdinova, B. L. Wadsworth, M. Flores, A. M. Beiler, E. A. Reyes Cruz, Y. Zenkov, G. F. Moore. *ACS Catal.* **8**, 9888 (2018).
[75] A. M. Beiler, D. Khusnutdinova, B. L. Wadsworth, G. F. Moore. *Inorg. Chem.* **56**, 12178 (2017).
[76] S. N. Karthick, K. V. Hemalatha, K. B. Suresh, F. Manik Clinton, S. Akshaya, H.-J. Kim. *Interfacial Engineering in Functional Materials for Dye-Sensitized Solar Cells*, John Wiley & Sons, Inc, Hoboken, NJ, p. 1 (2020).
[77] H. Tributsch. *Photochem. Photobiol.* **16**, 261 (1972).
[78] K. Hauffe, N. I. Ionescu, A. Meyer-Laack. *Naturwissenschaften* **59**, 165 (1972).
[79] L. L. Larina, E. M. Trukhan. *Zh. Fiz. Khim.* **53**, 1744 (1979).
[80] S. Hotchandani, P. V. Kamat. Chem. *Phys. Lett.* **191**, 320 (1992).
[81] B. O'Regan, M. Grätzel. *Nature* **353**, 737 (1991).
[82] G. J. Meyer. *ACS Nano* **4**, 4337 (2010).
[83] K. Sharma, V. Sharma, S. S. Sharma. *Nanoscale Res. Lett.* **13** (2018), https://doi.org/10.1186/s11671-018-2760-6.
[84] B. C. O'Regan, J. R. Durrant. *Acc. Chem. Res.* **42**, 1799 (2009).
[85] W. M. Campbell, K. W. Jolley, P. Wagner, K. Wagner, P. J. Walsh, K. C. Gordon, L. Schmidt-Mende, M. K. Nazeeruddin, Q. Wang, M. Gratzel, D. L. Officer. *J. Phys. Chem. C* **111**, 11760 (2007).
[86] A. Yella, H. W. Lee, H. N. Tsao, C. Y. Yi, A. K. Chandiran, M. K. Nazeeruddin, E. W. G. Diau, C. Y. Yeh, S. M. Zakeeruddin, M. Grätzel. *Science* **334**, 629 (2011).
[87] Y. C. Chang, C. L. Wang, T. Y. Pan, S. H. Hong, C. M. Lan, H. H. Kuo, C. F. Lo, H. Y. Hsu, C. Y. Lin, E. W. G. Diau. *Chem. Commun.* **47**, 8910 (2011).
[88] S. Mathew, A. Yella, P. Gao, R. Humphry-Baker, B. F. E. Curchod, N. Ashari-Astani, I. Tavernelli, U. Rothlisberger, M. K. Nazeeruddin, M. Grätzel. *Nat. Chem.* **6**, 242 (2014).
[89] K. Hu, R. N. Sampaio, J. Schneider, L. Troian-Gautier, G. J. Meyer. *J. Am. Chem. Soc.* **142**, 16099 (2020).
[90] S. N. Yun, N. Vlachopoulos, A. Qurashi, S. Ahmad, A. Hagfeldt. *Chem. Soc. Rev.* **48**, 3705 (2019).
[91] Y. Gong, S. Zhang, H. Gao, Z. Ma, S. Hu, Z. a. Tan. *Sustain. Energy Fuels* **4**, 4415 (2020).
[92] S. M. McCullough, J. M. Evans, T. Moot, A. D. Taggart, L. Troian-Gautier, J. F. Cahoon. *ACS Appl. Energy Mater.* **3**, 1496 (2020).
[93] M. Bonomo, D. Di Girolamo, M. Piccinni, D. P. Dowling, D. Dini. *Nanomaterials* **10**, 167 (2020).
[94] Y. M. Poronik, G. V. Baryshnikov, I. Deperasińska, E. M. Espinoza, H. Ågren, D. T. Gryko, V. I. Vullev. *Commun. Chem.* **3**, 190 (2020).
[95] A. Pecoraro, A. De Maria, P. Delli Veneri, M. Pavone, A. B. Munoz-Garcia. *Phys. Chem. Chem. Phys.* **22**, 28401 (2020).
[96] D. Ursu, M. Vajda, M. Miclau. *J. Alloys Compd.* **802**, 86 (2019).
[97] A. Sen, A. Gross. *ACS Appl. Energy Mater.* **2**, 6341 (2019).
[98] T. Bouwens, S. Mathew, J. N. H. Reek. *Faraday Discuss* **215**, 393 (2019).
[99] N. Zhang, J. Sun, H. Gong. *Coatings* **9**, 137/1 (2019), https://doi.org/10.3390/coatings9020137.
[100] J. Lu, Z. Liu, N. Pai, L. Jiang, U. Bach, A. N. Simonov, Y.-B. Cheng, L. Spiccia. *ChemPlusChem* **83**, 711 (2018).
[101] O. Langmar, C. R. Ganivet, P. Schol, T. Scharl, G. de la Torre, T. Torres, R. D. Costa, D. M. Guldi. *J. Mater. Chem. C* **6**, 5176 (2018).
[102] T. T. T. Pham, S. K. Saha, D. Provost, Y. Farre, M. Raissi, Y. Pellegrin, E. Blart, S. Vedraine, B. Ratier, D. Aldakov, F. Odobel, J. Boucle. *J. Phys. Chem. C* **121**, 129 (2017).

[103] E. M. Espinoza, B. Xia, N. Darabedian, J. M. Larsen, V. Nunez, D. Bao, J. T. Mac, F. Botero, M. Wurch, F. Zhou, V. I. Vullev. *Eur. J. Org. Chem.* **2016**, 343 (2016).
[104] Z. W. Wang, P. K. Nayak, J. A. Caraveo-Frescas, H. N. Alshareef. *Adv. Mater.* **28**, 3831 (2016).
[105] M. K. Brennaman, R. J. Dillon, L. Alibabaei, M. K. Gish, C. J. Dares, D. L. Ashford, R. L. House, G. J. Meyer, J. M. Papanikolas, T. J. Meyer. *J. Am. Chem. Soc.* **138**, 13085 (2016).
[106] O. Langmar, E. Fazio, P. Schol, G. de la Torre, R. D. Costa, T. Torres, D. M. Guldi. *Angew. Chem. Int. Ed.* **58**, 4056 (2019).
[107] K. A. Click, B. M. Schockman, J. T. Dilenschneider, W. D. McCulloch, B. R. Garrett, Y. Yu, M. He, A. E. Curtze, Y. Wu. *J. Phys. Chem. C* **121**, 8787 (2017).
[108] Y.-Z. Zheng, X. Tao, J.-W. Zhang, X.-S. Lai, N. Li. *J. Power Sources* **376**, 26 (2018).
[109] W. Shockley, H. J. Queisser. *J. Appl. Phys.* **32**, 510 (1961).
[110] S. Guo, D. Bao, S. Upadhyayula, W. Wang, A. B. Guvenc, J. R. Kyle, H. Hosseinibay, K. N. Bozhilov, V. I. Vullev, C. S. Ozkan, M. Ozkan. *Adv. Funct. Mater.* **23**, 5199 (2013).
[111] H. Lu, D. Bao, M. Penchev, M. Ghazinejad, V. I. Vullev, C. S. Ozkan, M. Ozkan. *Adv. Sci. Lett.* **3**, 101 (2010).
[112] D. Rehm, A. Weller. *Isr. J. Chem.* **8**, 259 (1970).
[113] D. Bao, B. Millare, W. Xia, B. G. Steyer, A. A. Gerasimenko, A. Ferreira, A. Contreras, V. I. Vullev. *J. Phys. Chem.* **113**, 1259 (2009).
[114] J. B. Derr, J. Tamayo, J. A. Clark, M. Morales, M. F. Mayther, E. M. Espinoza, K. Rybicka-Jasinska, V. I. Vullev. *Phys. Chem. Chem. Phys.* **22**, 21583 (2020).
[115] J. Wan, A. Ferreira, W. Xia, C. H. Chow, K. Takechi, P. V. Kamat, G. Jones, V. I. Vullev. *J. Photochem. Photobiol, A* **197**, 364 (2008).
[116] D. Bao, S. Ramu, A. Contreras, S. Upadhyayula, J. M. Vasquez, G. Beran, V. I. Vullev. *J. Phys. Chem. B* **114**, 14467 (2010).
[117] R. A. Marcus. *J. Chem. Phys.* **24**, 966 (1956).
[118] R. A. Marcus. *J. Chem. Phys.* **26**, 867 (1957).
[119] R. A. Marcus. *J. Chem. Phys.* **26**, 872 (1957).
[120] D. Meggiolaro, F. Ambrosio, E. Mosconi, A. Mahata, F. De Angelis. *Adv. Energy Mater.* **10**, 1902748 (2020).
[121] Y. Natanzon, A. Azulay, Y. Amouyal. *Isr. J. Chem.* **60**, 768 (2020).
[122] M. Scheele. *Z. Phys. Chem.* **229**, 167 (2015).
[123] I. G. Austin, N. F. Mott. *Adv. Phys.* **18**, 41 (1969).
[124] L. Landau. *Phys. Z. Sowjet Union* **3**, 664 (1933).
[125] S. I. Pekar. *Исследования по электронной теории кристаллов* (*Studies on the Electron Theory of Crystals*). Gosudarstvennoe Izdatel'stvo Tekh.-Teoret. Lit, Oak Ridge, TN (1951).
[126] S. Upadhyayula, D. Bao, B. Millare, S. S. Sylvia, K. M. M. Habib, K. Ashraf, A. Ferreira, S. Bishop, R. Bonderer, S. Baqai, X. Jing, M. Penchev, M. Ozkan, C. S. Ozkan, R. K. Lake, V. I. Vullev. *J. Phys. Chem. B* **115**, 9473 (2011).
[127] G. N. Chuev, V. D. Lakhno. *J. Theor. Biol.* **163**, 51 (1993).
[128] H. G. Ryu, M. F. Mayther, J. Tamayo, C. Azarias, E. M. Espinoza, M. Banasiewicz, L. G. Lukasiewicz, Y. M. Poronik, A. Jezewski, J. Clark, J. B. Derr, K. H. Ahn, D. T. Gryko, D. Jacquemin, V. I. Vullev. *J. Phys. Chem. C* **122**, 13424 (2018).
[129] A. Purc, E. M. Espinoza, R. Nazir, J. J. Romero, K. Skonieczny, A. Jeżewski, J. M. Larsen, D. T. Gryko, V. I. Vullev. *J. Am. Chem. Soc.* **138**, 12826 (2016).
[130] S. Upadhyayula, V. Nunez, E. M. Espinoza, J. M. Larsen, D. Bao, D. Shi, J. T. Mac, B. Anvari, V. I. Vullev. *Chem. Sci.* **6**, 2237 (2015).
[131] J. M. Vasquez, A. Vu, J. S. Schultz, V. I. Vullev. *Biotechnol. Prog.* **25**, 906 (2009).
[132] F. J. Ambrose, D. James. *Proc. Roy. Soc. Lond.* **61**, 316 (1897).
[133] G. Jones, D.-X. Yan, II, D. J. Gosztola, S. R. Greenfield, M. R. Wasielewski. *J. Am. Chem. Soc.* **121**, 11016 (1999).
[134] J. Hu, B. Xia, D. Bao, A. Ferreira, J. Wan, G. Jones, V. I. Vullev. *J. Phys. Chem.* **113**, 3096 (2009).
[135] G. Jones, D. Yan, II, J. Hu, J. Wan, B. Xia, V. I. Vullev. *J. Phys. Chem. B* **111**, 6921 (2007).
[136] S. J. Mora, E. Odella, G. F. Moore, D. Gust, T. A. Moore, A. L. Moore. *Acc. Chem. Res.* **51**, 445 (2018).
[137] S. Hammes-Schiffer. *Energy Environ. Sci.* **5**, 7696 (2012).
[138] S. Hammes-Schiffer. *Acc. Chem. Res.* **42**, 1881 (2009).
[139] J. D. Megiatto, D. D. Mendez-Hernandez, M. E. Tejeda-Ferrari, A. L. Teillout, M. J. Llansola-Portoles, G. Kodis, O. G. Poluektov, T. Rajh, V. Mujica, T. L. Groy, D. Gust, T. A. Moore, A. L. Moore. *Nat. Chem.* **6**, 423 (2014).
[140] A. Pannwitz, O. S. Wenger. *Dalton Trans.* **48**, 5861 (2019).
[141] E. Odella, B. L. Wadsworth, S. J. Mora, J. J. Goings, M. T. Huynh, D. Gust, T. A. Moore, G. F. Moore, S. Hammes-Schiffer, A. L. Moore. *J. Am. Chem. Soc.* **141**, 14057 (2019).
[142] W. D. Guerra, E. Odella, M. Secor, J. J. Goings, M. N. Urrutia, B. L. Wadsworth, M. Gervaldo, L. E. Sereno, T. A. Moore, G. F. Moore, S. Hammes-Schiffer, A. L. Moore. *J. Am. Chem. Soc.* **142**, 21842 (2020).
[143] Y. Yoneda, S. J. Mora, J. Shee, B. L. Wadsworth, E. A. Arsenault, D. Hait, G. Kodis, D. Gust, G. F. Moore, A. L. Moore, M. Head-Gordon, T. A. Moore, G. R. Fleming. *J. Am. Chem. Soc.* **143**, 3104 (2021).
[144] M. Krzeszewski, E. M. Espinoza, C. Cervinka, J. B. Derr, J. A. Clark, D. Borchardt, G. J. O. Beran, D. T. Gryko, V. I. Vullev. *Angew. Chem. Int. Ed.* **57**, 12365 (2018).

[145] D. Bao, S. Upadhyayula, J. M. Larsen, B. Xia, B. Georgieva, V. Nunez, E. M. Espinoza, J. D. Hartman, M. Wurch, A. Chang, C.-K. Lin, J. Larkin, K. Vasquez, G. J. O. Beran, V. I. Vullev. *J. Am. Chem. Soc.* **136**, 12966 (2014).
[146] R. A. Marcus. *Discuss. Faraday Soc.* **21** (1960).
[147] S. Yomosa. *Sup. Prog. Theor. Phys.* **40**, 249 (1967).
[148] J. B. Derr, J. Tamayo, E. M. Espinoza, J. A. Clark, V. I. Vullev. *Can. J. Chem.* **96**, 843 (2018).
[149] D. A. Doyle, J. M. Cabral, R. A. Pfuetzner, A. Kuo, J. M. Gulbis, S. L. Cohen, B. T. Chait, R. MacKinnon. *Science* **280**, 69 (1998).
[150] R. Dutzler, E. B. Campbell, M. Cadene, B. T. Chait, R. MacKinnon. *Nature* **415**, 287 (2002).
[151] Y.-G. K. Shin, M. D. Newton, S. S. Isied. *J. Am. Chem. Soc.* **125**, 3722 (2003).
[152] J. S. Richardson, D. C. Richardson. in *Prediction of Protein Structure and the Principles of Protein Conformation*, G. D. Fasman (Ed.), p. 1, Plenum, New York, NY (1989).
[153] L. Zubcevic, S.-Y. Lee. *Curr. Opin. Struct. Biol.* **58**, 314 (2019).
[154] J. Ludwiczak, A. Winski, A. M. da Silva Neto, K. Szczepaniak, V. Alva, S. Dunin-Horkawicz. *Sci. Rep.* **9**, 1 (2019).
[155] P. Kumar, M. Bansal. *FEBS J.* **282**, 4415 (2015).
[156] B. Xia, D. Bao, S. Upadhyayula, G. Jones, V. I. Vullev. *J. Org. Chem.* **78**, 1994 (2013).
[157] M. K. Ashraf, R. R. Pandey, R. K. Lake, B. Millare, A. A. Gerasimenko, D. Bao, V. I. Vullev. *Biotechnol. Prog.* **25**, 915 (2009).
[158] K. Rybicka-Jasinska, V. I. Vullev. *J. Photochem. Photobiol., A* **401**, 112779 (2020).
[159] K. Skonieczny, E. M. Espinoza, J. B. Derr, M. Morales, J. M. Clinton, B. Xia, V. I. Vullev. *Pure Appl. Chem.* **92**, 275 (2020).
[160] J. B. Derr, K. Rybicka-Jasińska, E. M. Espinoza, M. Morales, M. K. Billones, J. A. Clark, V. I. Vullev. *Biomolecules* **11**, 429 (2021).
[161] J. M. Larsen, E. M. Espinoza, J. D. Hartman, C.-K. Lin, M. Wurch, P. Maheshwari, R. K. Kaushal, M. J. Marsella, G. J. O. Beran, V. I. Vullev. *Pure Appl. Chem.* **87**, 779 (2015).
[162] E. M. Espinoza, J. M. Larsen, V. I. Vullev, J. Phys. *Chem. Lett.* **7**, 758 (2016).
[163] J. M. Larsen-Clinton, E. M. Espinoza, M. F. Mayther, J. Clark, C. Tao, D. Bao, C. M. Larino, M. Wurch, S. Lara, V. I. Vullev. *Phys. Chem. Chem. Phys.* **19**, 7871 (2017).
[164] J. M. Larsen, E. M. Espinoza, V. I. Vullev. *J. Photon. Energy* **5**, 1, 055598 (2015).
[165] E. M. Espinoza, J. M. Larsen, V. I. Vullev. *ECS Trans.* **66**, 1 (2015).
[166] E. M. Espinoza, V. I. Vullev. *ECS Trans.* **77**, 1517 (2017).
[167] E. M. Espinoza, J. A. Clark, J. Soliman, J. B. Derr, M. Morales, V. I. Vullev. *J. Electrochem. Soc.* **166**, H3175 (2019).
[168] J. B. Derr, J. A. Clark, M. Morales, E. M. Espinoza, S. Vadhin, V. I. Vullev. *RSC Adv.* **10**, 24419 (2020).